

Performance Analysis of a GPS Equipment



M. Filomena Teodoro, Fernando M. Gonçalves, and Anacleto Correia

Abstract In emerging economies the easiest way to ensure the geodetic support still is the static relative positioning (SRP) using a single reference station. This technique provides surveyors the ability to determine the 3D coordinates of a new point with centimeter-level accuracy. The objective of this work is to evaluate GPS SRP regarding accuracy, as the equivalent of a real time kinematic (RTK) network and to address the practicality of using either a continuously operating reference stations (CORS) or a passive control point for providing accurate positioning control. The precision of an observed 3D relative position between two global navigation satellite systems (GNSS) antennas, and how it depends on the distance between these antennas and on the duration of the observing session, was studied. We analyze the performance of the software for each of the six chosen ranges of length in each of the four scenarios created, considering different intervals of observation time. An intermediate inference level technique (Tamhane and Dunlop, *Statistics and data analysis: from elementary to intermediate*, Prentice Hall, New Jersey, 2000), an analysis of variance, establishes the evidence of relation between observing time and baseline length.

M. F. Teodoro (✉)

CINAV, Center of Naval Research, Naval Academy, Almada, Portugal

CEMAT, Center for Computational and Stochastic Mathematics, Instituto Superior Técnico, Lisbon University, Lisboa, Portugal

e-mail: maria.alves.teodoro@marinha.pt

F. M. Gonçalves

NGI, Nottingham Geospatial Institute, University of Nottingham, Nottingham, UK

A. Correia

CINAV, Center of Naval Research, Naval Academy, Almada, Portugal

e-mail: cortez.correia@marinha.pt

© Springer International Publishing AG, part of Springer Nature 2018

T. A. Oliveira et al. (eds.), *Recent Studies on Risk Analysis*

and *Statistical Modeling*, Contributions to Statistics,

https://doi.org/10.1007/978-3-319-76605-8_21

1 Introduction

RTK networks are common in Europe but this is not the case in emerging economies where huge construction projects are running requiring geodetic support. In such cases, the easiest way to ensure that kind of support still is the SRP using a single reference station. This technique provides surveyors the ability to determine the 3D coordinates of a new point with centimeter-level accuracy relative to a control point located several hundred kilometers away, which in turn can be associated with another GNSS receiver of a CORS operated by some institution.

Today the global navigation satellite systems play a fundamental role in the way that surveyors measure positional coordinates. It is now possible to determine the 3D coordinates of a new point with centimeter-level accuracy relative to a control point located several hundred kilometers away, which in turn can be associated with another GNSS receiver of a CORS operated by some institution. Examples of such networks are the ordnance survey (OS) Network across the UK [14] or, globally, the International GNSS Service Network [7].

With the implementation of real time networks (RTN), particularly across Europe and North America, the way surveyors work has dramatically changed over the last few years. Certainly, the growth of RTN will continue and it is expected that in the near future the work taking place in areas covered by these infrastructures will be dominated by RTK techniques. However, in other regions of the world which can become, or already are, of interest for scientific or industry projects, this type of infrastructure does not exist. Consequently, “old” methods such as the static observation and post processing continue to play a prominent role in GNSS surveying in order to provide accurate position solutions without support of network corrections. Furthermore, when surveyors decide which GNSS methods to use, they must consider several aspects of a project. Besides specific requirements from clients, other important factors to be considered are budget, schedule, accuracy, and control over how data is managed.

In this research the coordinates of the OS active stations were used as “true” values to address the practicality of using either a CORS or a passive control point for providing accurate positioning control and, implicitly, the performance of the software used. The precision of an observed 3D relative position between two GNSS antennas, and how it depends on the distance between these antennas and on the duration of the observing session, was studied. These results were attained through using commercial software LGO to process 105 single baselines, ranging from 61 to 898 km, according to observing sessions of varying lengths. ABEP was used as a reference station, with fixed coordinates, and the values obtained for the rover stations compared with those provided by OS. Also, to address the differences between using broadcast or precise ephemerides and computing the tropospheric effects or for simply applying a tropospheric model, the data processing was repeated for all different strategies.

Generally results show, whatever the strategy followed, that the length of the baseline matters, regarding the rate of successful baselines processed for a priori

given values of 1D (ellipsoidal height accuracy) and 2D (compound of longitude and latitude accuracy). While distance matters, under the conditions of this experiment, the results also indicate that the duration of the observing session does not present the same pattern for 1D and 2D. In addition to the length of the baseline and the duration of the observing session, positioning precision depends on several other factors, including the methodology and the software used for processing GPS data, in this case the LGO. Biases associated with meteorological effects (ionosphere and troposphere) also play an important role in the total error budget of positioning precision.

This work investigates the performance of commercial software LGO when processing baselines in static mode. The parameter to be tested is the time of observation needed to achieve a given accuracy (1D and 2D) for a set of ranges of baseline lengths. Four different scenarios were created, as follows:

- Broadcast ephemerides and Hopfield model (BH);
- Broadcast ephemerides and Computing the troposphere (BC);
- Precise ephemerides and Hopfield model (PH);
- Precise ephemerides and Computing the troposphere (PC).

Summarizing, the present work is comprised of introduction and conclusion sections, a section with background information, another describing the data and the methodology adopted and two sections containing specific tests and results.

2 GNSS Overview

In this section, we provide an introduction of GPS, the navigation system used in this research. As there are a number of relevant references available, e.g. [4, 9, 10], only a very brief discussion on the basics of the system will be given, with particular emphasis on the parts which are relevant to observation modeling of systematic biases and errors affecting GPS measurements. The various types of GPS observables of interest on baseline determination in SRP are also described, as are some of their possible combinations. The possible usefulness of Precise Ephemerides, in terms of the increased accuracy in long baselines, is also evaluated.

There are numerous sources of measurement errors that influence GPS performance. Both observables types, code and phase, are affected by many systematic biases and errors, different in their source and suitable method of treatment. The most important of these biases and errors are briefly reviewed here. The orbital errors and tropospheric effects will be discussed later with more detail.

Finally, because tropospheric delay is a dominant factor for the relative positioning accuracy in GPS/GNSS long baselines, as the LGO strategy using the “ionospheric-free observable” almost removes all first-order ionospheric biases, a description of the different strategies available to mitigate tropospheric biases is also provided. Differences between the Hopfield model and tropospheric computing techniques are highlighted.

2.1 *Systematic Biases and Errors*

There are numerous sources of measurement errors that influence GPS performance. Both observables types, code and phase, are affected by many systematic biases and errors, different in their source and suitable method of treatment. The most important of these biases and errors are briefly reviewed here. The orbital errors and tropospheric effects will be discussed later with more detail.

The sum of all systematic biases and errors contributing to the measurement error is referred to as a range bias. Bingley in [2] argues that this bias is caused by a physical phenomenon, as is the case, for example, in ionospheric or tropospheric delays, and error is the quantity remaining after the bias has been mitigated to some extent, which is the case, for example, for errors in broadcast ephemerides. According to the same author, the systematic biases and errors affecting GPS measurements can be grouped into three main categories: satellite related, atmospheric related, and station related.

2.2 *Satellite Related Biases and Errors*

Satellite related biases consist of biases of satellite ephemerides (orbital errors), satellite clock offsets and satellite antenna phase centers, as the selective availability (SA) was internationally terminated by the US Government in May 1, 2000.

The error in satellite coordinates is the difference between the predicted and the “true” satellite position. The predicted position is estimated by the Master Control Stations (MCS), using data collected by Master Stations (MS), and uploaded to the satellites, which in turn broadcast that information to users through the navigation message. The predicted satellite position is currently on the order of 1 m [2]. Besides broadcast ephemerides, precise ephemerides are available from IGS [7], providing an accuracy of 2.5 cm in their rapid and final format.

Although, precise as they are, satellites clocks are not perfect. The satellite clock error is defined as the difference between satellite clock time and true GPS time. The MCS computes and broadcasts to the users the parameters to correct the satellite clock error, according to the equation in [4, p. 52].

Because GPS orbit is calculated with respect to the satellite’ center of mass but the observation refers to the antenna phase center (point of transmission), which are not coincident, the offset between these two centers has to be known. In addition to this, at the point of transmission, the electrical center is not the geometrical center. By applying Phase Center Offsets (PCO) and Phase Center Variations (PCV) corrections it is possible to relate the measurements consistently to the satellite’s center of mass. In [11] the author states that in global networks absolute PCVs have to be taken into account due to the fact that the GPS satellites are normally seen at different elevations from the ends of a baseline.

2.3 *Atmospheric Related Biases and Errors*

Atmospheric biases are due to ionospheric and tropospheric delays. The ionospheric bias is caused by the propagation of the GPS signals in the ionosphere, which is the region of the atmosphere between about 50 and 1000 km above the Earth surface. Within this region ions and free electrons, originating in sun radiation, are present in quantities that affect the propagation of electromagnetic signals. In the GPS case, the code (pseudo-range) is delayed and the carrier phase is advanced. Because this is a dispersive medium at GPS frequencies, i.e., the propagation speed depends on the carrier frequency, resolution of ionospheric delays can be accomplished by using a dual-frequency receiver. However, according to Wells in [18], during a high solar activity cycle (e.g., solar maximum between 2011 and 2013) and in mid afternoons this technique may not be adequate for certain applications. The ionospheric delay depends on the Total Electron Content (TEC) along the signal path and on the frequency used [6]. The ionospheric bias may range from 5 (at night, the satellite at the zenith) to 150 m (at midday and the satellite at low elevation) [18].

The troposphere is the lowest atmosphere layer, from the Earth's surface to 50 km. The tropospheric delay is caused by the refraction of the GPS signal in this layer. This bias depends on parameters such as the temperature, humidity, and pressure. It varies with the height of the station. Unlike the ionosphere, this is a non-dispersive medium for GPS frequencies, that is, the delay is independent from the carrier frequency, so that dual-frequency receivers cannot be used to eliminate it. In GPS case both pseudo-range and carrier phase will experiment the same delay. Usually, the tropospheric bias is broken in two components [5]:

A hydrostatic component, including about 80–90% of the error and highly predictable, according to atmospheric pressure and temperature, and satellite' elevation angle.

A wet component, including about 10–20% of the error, is more difficult to predict, due to variations of the partial water vapor on the atmosphere.

A number of studies have been performed to create tropospheric models to mitigate the influence of this bias, among them the Hopfield model, used in this research. The hydrostatic, or dry, component can be precisely described by these models with an accuracy of $\pm 1\%$, while the wet component can be modeled by surface weather data to within 3–4 cm [18]. Besides using models, usually based on meteorological parameters, other approaches to determine the wet component include direct measurement with water vapor radiometers and the use of a station-dependent zenith scale factor for each satellite pass [12].

2.4 Station Related Biases and Errors

Station related biases and errors to be considered include those related to the equipment (receiver clock offset and receiver antenna phase centers) and location of the station (multipath and geophysical phenomena).

The receiver clock error is the difference between the time maintained by the receiver clock and the reference GPS time. Differencing observations between satellites can eliminate the receiver clock error. This procedure is based on the assumption that the clock bias is independent at each measurement time. “In the case of relative positioning, such as static positioning using carrier phase, the receiver clock offsets are eliminated, with the assumption that a receiver appears to make observations to all satellites at the same time” [2].

Receiver Antenna Phase centers biases are the compound of PCOs and PCVs. PCO is the offset between the point of reception (mean phase center), at the antenna, and the physical Antenna Reference Point (ARP). This offset is constant, for each antenna and frequency, whereas PCVs vary depending on the direction (azimuth and elevation of the satellite) and frequency of the transmitting signal. According to [2], if not accounted for, the bias due to these variations can reach several centimeters in the observed carrier phase for some types of antenna. For high accurate applications, in static positioning using carrier phase, these biases have to be mitigated. Some procedures should then be followed, in order to eliminate or reduce this type of bias, such as the use of similar antennas (choke ring, if possible), directed north on both sides of the baseline. Nevertheless, even in the case of similar antennas being used, models for receiver antenna phase centers (particularly PCVs) must be applied for baselines greater than 100 km [2].

Multipath is the phenomena whereby a signal arrives at a receiver from more than one path because of the reflections during the signal propagation. As the bias due to multipath is wavelength dependent, code and carrier phase are affected in different ways. Pseudo-range multipath can reach up to one chip length of the PRN codes (293 m for C/A code and 29.3 m for P code). Carrier phase measurements are not free from multipath either, although the effect is about two orders of magnitude smaller than in pseudo-ranges (e.g. 5 cm for L1), it contributes to the phase measurement noise [3]. Furthermore, because multipath affects L1 and L2 signals differently, this can cause problems during cycle slip detection and correction [2]. For static positioning using carrier phase, as demonstrated in [13], multipath signature can be detected through the analysis of strong correlation present in the adjustment’ residuals of two consecutive sidereal days, due to the geometry repetition of satellite-antenna-reflector.

Applying models for geophysical phenomena, such as the solid earth tides (SET) or ocean tide loading (OTL) is important when striving for centimeter-level accuracies using carrier phase relative positioning over long baselines lengths.

3 Data and Methodology

OS' active stations were used to investigate the relation between time of observation and length of the baseline. A total of 105 baselines were processed using LGO, separated into six range groups (R_i , $i = 1, \dots, 6$) according to their lengths in kilometers:

- $R_1 = [000 - 100] \rightarrow (5 \text{ baselines})$
- $R_2 = [100 - 200] \rightarrow (14 \text{ baselines})$
- $R_3 = [200 - 300] \rightarrow (27 \text{ baselines})$
- $R_4 = [300 - 400] \rightarrow (29 \text{ baselines})$
- $R_5 = [400 - 500] \rightarrow (14 \text{ baselines})$
- $R_6 = [500 - 900] \rightarrow (16 \text{ baselines})$

All the stations are permanent stations of clear sky visibility and with low multipath conditions. The quality of the data is therefore expectantly high. Day 13/06/2013 of receiver independent exchange (RINEX) data of GPS week 1744 was downloaded from the data archive of the active GPS network of Ordnance Survey (OS Net) for each of the 106 stations [15]. These RINEX data include phase measurement of the carrier waves L_1 and L_2 , P_1 , P_2 and C/A pseudo-range code at a 30 s interval.

For this experiment, 24 h of dual-frequency GPS carrier phase observations for each of 105 baselines formed by ABEP, chosen as reference station, and all the other active stations, designated as rover, from OS Network were used. These 105 baselines range in length from 61 to 898 km and correspond to all active stations considered "healthy" on 13/06/2013. The data for each baseline comprised the same 24-h session that was further subdivided into periods of time of 1, 2, 3, 4, 6, 8, 12, and 24 h as follows, where the two first digits represent the beginning of the observation period and the last two the end:

- 1 h periods: [0001], [0607], [1213], [1819];
- 2 h periods: [0002], [0608], [1214], [1820];
- 3 h periods: [0003], [0609], [1215], [1821];
- 4 h periods: [0004], [0408], [0812], [1216], [1620], [2024];
- 6 h periods: [0006], [0612], [1218], [1824];
- 8 h periods: [0008], [0816], [1624];
- 12 h periods: [0012], [1224];
- 24 h period: [0024].

The division of time in this way was done in order to evaluate the performance of the software for different lengths of observation time.

The criteria followed to select the reference station were primarily based on location. Thus ABEP, on the west coast of England, was chosen, because of its high altitude and location, providing a well-distributed range of radial vectors to all the other active stations, either in latitude and longitude. Its 3D positional coordinates were fixed to the official values adopted by OS.

In order to evaluate at what range of baseline lengths the use of precise ephemerides becomes worthwhile, both results using broadcast and precise ephemerides are presented as well. The corresponding SP3 files were downloaded from the data archive of IGS [8]. These include precise ephemerides at a sampling interval of 15 min and the high-rate precise satellite clocks with a sampling of 30 s.

Hence, the four different scenarios can be compared as follows:

- Direct comparison of the results obtained using the broadcast ephemerides and the precise ephemerides (BH versus PH and BC versus PC);
- Direct comparison of the results obtained using Hopfield model and computing the troposphere (BH versus BC and PH versus PC).

At starting points 1D, 2D, and 3D accuracy criteria were established for each baseline, as only successful processed baselines are of interest for this research. The chosen values were set to 1D and 2D accuracies to be better than 3 cm and 3D better than 4.5 cm. These are realistic values, as the OS active stations have 1D accuracy of about 2 cm in magnitude and close to 1 cm in 2D. Therefore, assuming the 3 cm as 1D and 2D threshold seems to be reasonable due to the fact that this tolerance allows for the “absorption” of errors inherent to the coordinates of the stations. Despite how perfectly the baseline was calculated an error of up to 4 cm in height and 2 cm in plan could arise due to the uncertainty associated with the coordinates.

The published coordinates of each of these stations (in Cartesian format on the header of the corresponding RINEX file) are assumed as “true” and used to compute the errors (1D, 2D, and 3D) in the solutions processed by LGO.

Figure 1 presents the percentage of successful baselines per range in 1D (black) and 2D (blue). There is a clear trend for fewer successful baselines as the length increases, either in 1D or 2D.

In Fig. 2, where the results are organized in a detailed form (each rectangle contains the eight box-plots, relatively to four strategies for 1D and 2D per range length), the trend is evident in all cases. In Table 1 we present the percentage of successful baselines per range in 1D (black) and 2D (blue) and per strategy. It is also easily to detect such behavior. That is a clear trend for a lower quantity of successful baselines as the length increases, regardless of the strategy adopted, either in 1D or 2D.

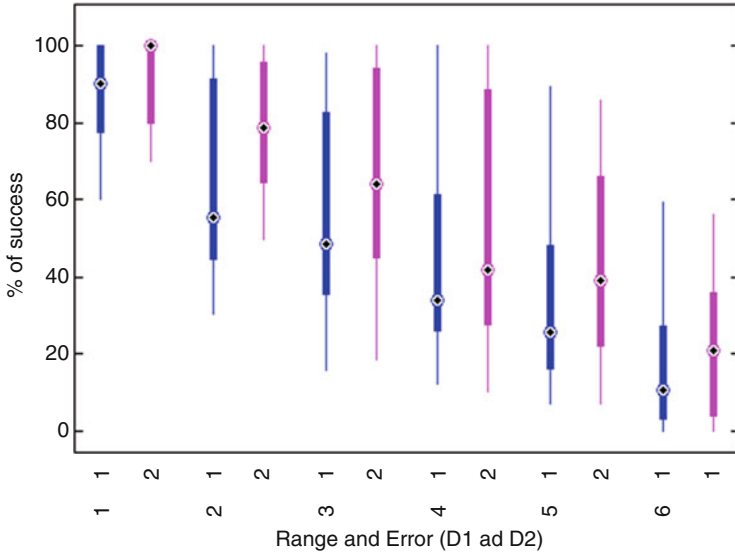


Fig. 1 Percentage of successful baselines distinct ranges (R_i , $i = 1, \dots, 6$) in 1D (in blue) and 2D (in magenta)

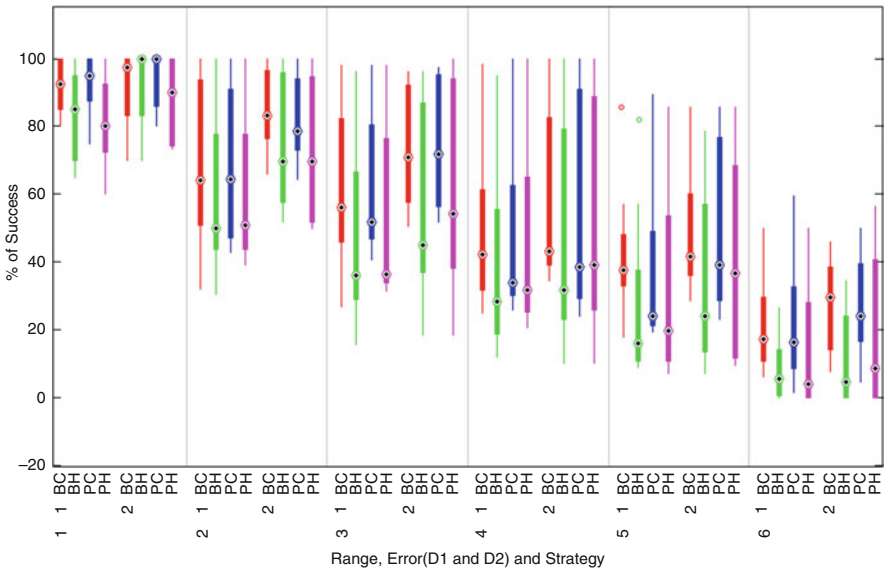


Fig. 2 Percentage of successful baselines distinct ranges (R_i , $i = 1, \dots, 6$) in 1D (rectangle left side) and 2D (rectangle right side) for strategies BH (in red), BC (in green), PH (in blue), and PC (in magenta)

Table 1 Averaged percentage of successful baselines in 1D and 2D for total (T) and distinct ranges ($R_i, i = 1, \dots, 6$)

Strategies	Processed	Pass	T	R_1	R_2	R_3	R_4	R_5	R_6
BH	2940	880	29.932	77.143	53.571	37.434	27.094	13.520	1.339
	2940	1756	59.728	97.145	83.418	71.296	60.099	44.643	20.537
BC	2940	1379	46.905	82.857	70.663	57.804	38.424	34.949	22.321
	2940	1875	63.776	98.571	82.908	76.190	65.394	49.235	25.000
PH	2940	840	28.571	72.857	50.510	37.302	25.739	11.990	0.223
	2940	2055	69.898	97.143	84.184	81.746	73.153	59.694	32.143
PC	2940	1206	41.020	84.286	66.582	54.365	28.818	27.296	16.518
	2940	2087	70.986	100.000	84.439	83.466	73.522	59.184	35.045

Strategies BH, BC, PH, and PC. Percentage of success for 1D in black; for 2D in blue
 Four strategies considering 1D and 2D

In a preliminary approach, it was found that the different ranges led to significantly different results. Were used parametric tests to compare proportions (t-test). With some small samples in certain ranges, were also applied some nonparametric tests that allow us to compare location measures, or a chi-square test and a Kruskal-Wallis to evaluate if the proportions of success are the same in the different ranges; a chi-square independence test was also used to evaluate the relation between the proportion of success and range. In Table 2 are the p -values obtained when the differences of the proportions of success for different ranges and strategies are tested.

In general, different strategies conduce to similar results: almost all comparisons have the same conclusion—the proportions of success in different ranges are not equal except when the ranges are sequential of each other. Also were performed similar tests comparing different strategies considering the same range. Generally, the proportions of success for the same range, but with different strategies conducted to significant tests, meaning that there is statistical evidence of different proportions of success per different strategies for same range. These conclusions are visible in Fig. 2.

We also performed an analysis of variance with four factors (parametric and non-parametric approach). The results of such analysis are similar for both cases: generally each factor is significant, meaning that the probability for success is not equal for each level of the considered factor. The intersection of each factor with the other considering secondary and third level intersections was not significant. The resume of that analysis can be found in Fig. 3. In this study we have merged the classes with smaller exposure time. The level 3 of factor duration means exposure time until 3 h.

We also performed the Scheffe’s S procedure, derived from F Distribution. This technique provides a simultaneous confidence level for comparisons for all linear combinations of means, namely for comparisons of simple differences of pairs. Figure 4 illustrates such comparisons for all levels of each factor. The conclusions are similar.

Table 2 Tests for difference of success probability for distinct ranges

Strategies	Ranges	R_2	R_3	R_4	R_5	R_6
BH	R_1	0.3204	0.0679	0.0204	0.0073	0.0008
		0.1129	0.3127	0.6257	0.9886	0.5567
	R_2		0.3271	0.0988	0.0200	0.0007
			0.1115	0.0096	0.0126	0.0004
	R_3			0.4097	0.0745	0.0006
				0.2769	0.1261	0.0099
	R_4				0.2767	0.0052
					0.4756	0.0827
BC	R_1	0.5652	0.2053	0.0267	0.0367	0.0065
		0.1864	0.0291	0.0029	0.0032	0.0000
	R_2		0.4100	0.0395	0.0530	0.0054
			0.6076	0.1981	0.0545	0.0005
	R_3			0.1452	0.1585	0.0158
				0.3743	0.0934	0.0005
	R_4				0.8250	0.2491
					0.3190	0.0060
PH	R_1	0.3640	0.1159	0.0357	0.0122	0.0017
		0.3059	0.1534	0.0383	0.0237	0.002
	R_2		0.4222	0.1208	0.0229	0.0008
			0.8434	0.3924	0.1420	0.0019
	R_3			0.3533	0.0538	0.0003
				0.4418	0.1514	0.0009
	R_4				0.2541	0.0033
					0.3896	0.0063
PC	R_1	0.4018	0.1237	0.0048	0.0116	0.0018
		0.1266	0.0278	0.0028	0.0064	0.0000
	R_2		0.4451	0.0168	0.0320	0.0034
			0.9360	0.3946	0.1339	0.0033
	R_3			0.0502	0.0844	0.0071
				0.3645	0.1125	0.0012
	R_4				0.9174	0.3316
					0.3598	0.0110
					0.4812	
					0.1845	

Strategies BH, BC, PH, and PC. P -values for 1D in black; P -values for 2D in blue
 Four strategies considering 1D and 2D

Analysis of Variance					
Source	Sum Sq.	d. f.	Mean Sq.	F	Prob>F
Range	196068.7	5	39213.7	102.22	0
Strategy	9323.3	3	3107.8	8.1	0
PrecisionD1D2	2649.9	1	2649.9	6.91	0.0089
Duration	37693.4	5	7538.7	19.65	0
Error	141552.6	369	383.6		

Constrained (Type III) sums of squares.

Fig. 3 Analysis of Variance (four factors)—Percentage of successful baselines distinct ranges (R_i , $i = 1, \dots, 6$); Duration of Exposure; Strategies BH, BC, PH, PC; Precision (1D and 2D)

4 Discussion of Results, Conclusions, and on Going Work

This work studies the relation for single baselines between lengths ranges and between the different ranges and the observation time required to obtain high-accurate positioning, using commercial software LGO. A brief analysis for different amplitudes of time interval of exposure, considering the four strategies is reproduced partially in this paper. The results are valid for this specific software and under the conditions of the experiments. Four different strategies were established and evaluated through the processing of a total of 11,760 baselines. The data processing and testing used several options concerning the best thresholds for accuracy. The LGO results were compared with the published coordinates by Ordnance Survey and the baselines passing the accuracy criteria were isolated. The division of time in this way was done in order to evaluate the performance of the software for different lengths of observation time. It revealed that the largest amplitude of time exposure interval, the bigger percentage of success.

Clearly was shown the dependence of success in 1D regarding the baseline length. No matter the strategy adopted, broadcast or precise ephemerides, Hopfield model or computing the troposphere, the rate of successful baselines processed decreases as the baseline length increases, following a linear trend. Generally, when looking at the range 1 to range 3 baseline length classes, BC performance is slightly better than PC but it is absolutely certain that computing the troposphere leads to higher rates of success for these three classes (BC vs BH and PC vs PH). Using LGO to process individual longer baselines (range 4 to range 6 classes), without any kind of redundancy, represents a risk, as the percentage of success is always less than 50 %.

A preliminary experiment shows that to obtain high accurate relative positioning 3D coordinates for long baselines in static mode with LGO at least 4 h of observation are recommended. Therefore, it is important to give, in a short time, a special focus to periods of this magnitude and over. These cover the whole day in nonoverlapping periods, whereas for the 1, 2 and 3 h intervals only representative samples were chosen. It is still need to analyze the results from similar lengths but at different times of the day experiencing diverse atmospheric conditions. Other tests and

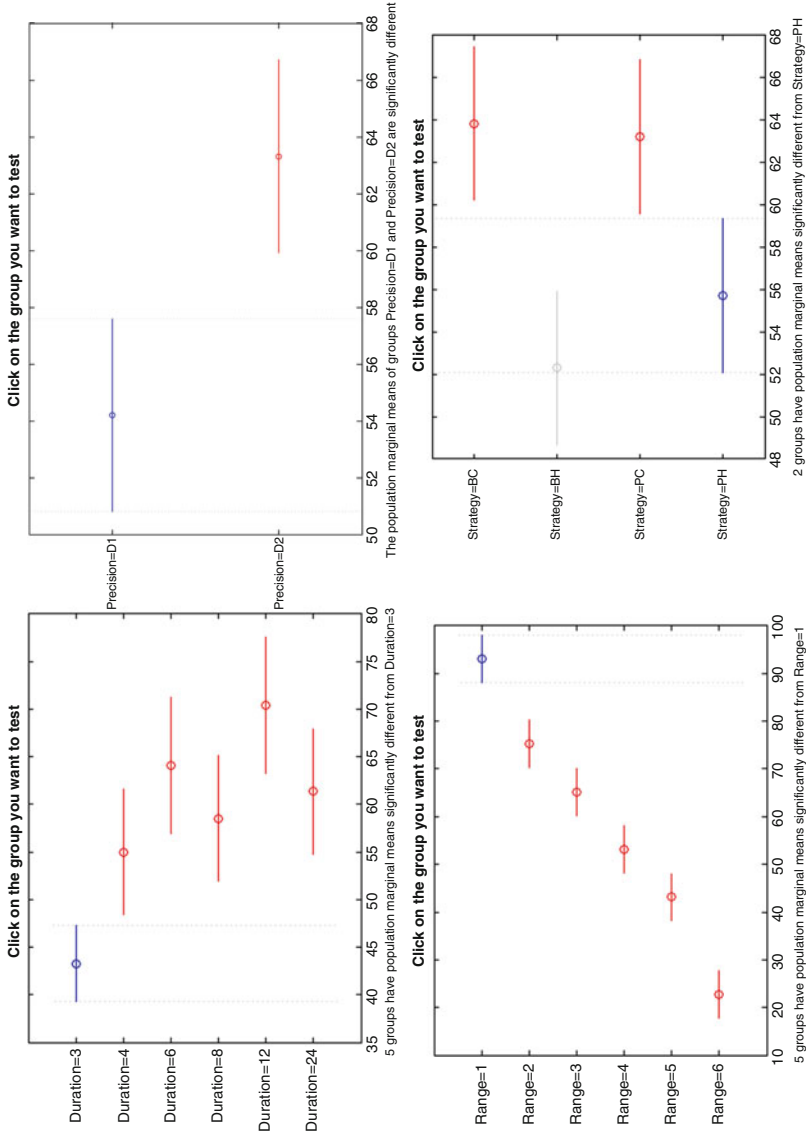


Fig. 4 Scheffe simultaneous mean percentage of successful baselines confidence intervals for the each factor levels—Duration of Exposure (top-left); Precision 1D and 2D (top-right); distinct ranges R_i , $i = 1, \dots, 6$ (bottom-left); Strategies BH, BC, PH, PC (bottom-right)

techniques, inquiring about the significance of the hour of the day, the amplitude of time interval of exposure, considering the four strategies.

An Analysis of Variance with several factors [16] (range, strategies, amplitude of interval time of exposure) was applied. Another possible approach is to model the data by General Linear Models [1, 17]. Such statistical approach details will be found in a future continuation of this manuscript.

Acknowledgements This work was supported by Portuguese funds through the *Center for Computational and Stochastic Mathematics (CEMAT)*, *The Portuguese Foundation for Science and Technology (FCT)*, University of Lisbon, Portugal, project UID/Multi/04621/2013, and *Center of Naval Research (CINAV)*, Naval Academy, Portuguese Navy, Portugal.

References

1. Anderson, T.W.: *An Introduction to Multivariate Analysis*. Wiley, New York (2003)
2. Bingley, R.M.: *GNSS principles and observables: systematic biases and errors*. Short Course, University of Nottingham, Nottingham Geospatial Institute (2013)
3. Georgiadou, Y., Kleusberg, A.: Multipath effects in static and kinematic GPS surveying. In: *Global Positioning System: An Overview*. International Association of Geodesy Symposia, vol. 102, pp. 82–89. Springer, Heidelberg (2002)
4. Hofmann-Wellenhof, B., Lichtenegger, H., Wasle, H.: *GNSS-Global Navigation Satellite Systems: GPS, GLONASS, Galileo, and More*. Springer Verlag-Wien, New York (2008)
5. Hopfield, H.S.: Tropospheric effect on electromagnetically measured range: prediction from surface weather data. *Radio Sci.* **6**(3), 357–367 (1971)
6. Hoque, M.M., Jakowski, N.: Ionospheric propagation effects on GNSS signals and new correction approaches. In: Shuanggen, J. (ed.) *Global Navigation Satellite Systems: Signal, Theory and Applications*, pp. 381–405. InTech, Rijeka (2012). <https://doi.org/10.5772/30090>
7. IGS: International GNSS Service. <http://igsceb.jpl.nasa.gov/> (2016). Accessed 19 Aug 2016
8. IGS: International GNSS Service. http://igsceb.jpl.nasa.gov/components/prods_cb.html (2016). Accessed 19 Aug 2016
9. Kaplan, E.D., Hegarty, C.J.: *Understanding GPS: Principles and Applications*. Artech House, Norwood (2006)
10. Leick, A.: *GPS Satellite Surveying*. Wiley, New Jersey (2004)
11. Mader, G.L.: GPS antenna calibration at the national geodetic survey. *GPS Solutions* **3**(1), 50–58 (1999)
12. Mendes, V.B.: *Modeling the neutral-atmosphere propagation delay in radiometric space techniques*. PhD thesis, University of New Brunswick (1999)
13. Meng, X.: *Modeling the neutral-atmosphere propagation delay in radiometric space techniques*. PhD thesis, University of Nottingham (2002)
14. OS Net Business and Government. Ordnance survey. <http://www.ordnancesurvey.co.uk/oswebsite/products/os-net/index.html> (2016). Accessed 19 Aug 2016
15. OS Net Business and Government. Ordnance survey. <http://www.ordnancesurvey.co.uk/gps/os-net-rinex-data/> (2016). Accessed 19 Aug 2016
16. Tamhane, A.C., Dunlop, D.D.: *Statistics and Data Analysis: From Elementary to Intermediate*. Prentice Hall, New Jersey (2000)
17. Turkman, M.A., Silva, G.: *Modelos Lineares Generalizados da Teoria a Prática*. Sociedade Portuguesa de Estatística, Lisboa (2000)
18. Wells, D.E., et al.: *Guide to GPS Positioning*. Canadian GPS Associates, Fredericton. http://plan.geomatics.ucalgary.ca/papers/guide_to_gps_positioning_book.pdf (1986). Accessed 1 Oct 2016